PAPER

Qubit coupled cluster singles and doubles variational quantum eigensolver ansatz for electronic structure calculations

View the article online for updates and enhancements.

Quantum Science and Technology

Qubit coupled cluster singles and doubles variational quantum eigensolver ansatz for electronic structure calculations

Rongxin Xia[ID] and Sabre Kais[*][ID]

Department of Chemistry, Department of Physics and Astronomy, and Purdue Quantum Science and Engineering Institute, Purdue University, West Lafayette, United States of America
[*] Author to whom any correspondence should be addressed.

E-mail: kais@purdue.edu

Abstract

Variational quantum eigensolver (VQE) for electronic structure calculations is believed to be one major potential application of near term quantum computing. Among all proposed VQE algorithms, the unitary coupled cluster singles and doubles excitations (UCCSD) VQE ansatz has achieved high accuracy and received a lot of research interest. However, the UCCSD VQE based on fermionic excitations needs extra terms for the parity when using Jordan–Wigner transformation. Here we introduce a new VQE ansatz based on the particle preserving exchange gate to achieve qubit excitations. The proposed VQE ansatz has gate complexity up-bounded to $O(n^4)$ for all-to-all connectivity where n is the number of qubits of the Hamiltonian. Numerical results of simple molecular systems such as BeH_2, H_2O, N_2, H_4 and H_6 using the proposed VQE ansatz gives very accurate results within errors about 10^{-3} Hartree.

1. Introduction

Quantum computing has been developing rapidly in recent years as a promising new paradigm for solving many problems in science and engineering. One major potential application of quantum computing is solving quantum chemistry problems [1] such as electronic structure of molecules, which has received a lot of research interest and achieved a big success in both algorithmic development and experimental implementation. The early development of electronic structure calculations was based on the quantum phase estimation algorithm developed by Kitaev [2], Abrams and Lloyd [3] and used to find spectrum of simple molecular systems [4–9]. More recently, hybrid classical-quantum algorithms have been developed such as the variational quantum eigenslover (VQE) [10–13] and quantum machine learning techniques [14] for electronic structure calculations. Moreover, many experiments have been conducted on quantum computers to show that electronic structure calculations of simple molecules are possible on current Noisy Intermediate-Scale Quantum (NISQ) devices [15–17].

One of the most promising quantum algorithms to perform electronic structure calculations is based on unitary coupled cluster [18] singles and doubles (UCCSD), which implements the quantum computer version of UCCSD as the VQE ansatz [10, 19, 20] to calculate the ground state from a Hartree–Fock reference state. The results from UCCSD VQE achieve high accuracy [1, 19, 21, 22]. However, the gate complexity for first order trotterization UCCSD VQE is up-bounded to $O(n^5)$ [1, 19] using Jordan–Wigner transformation where n is the number of qubits of the Hamiltonian. This makes it difficult to implement on current NISQ devices. Some strategies developed may be used to reduced the complexity, for example, the ordering and parallelization techniques in [23] can reduce the circuit depth by $O(n)$ [19] and low-rank factorization [24] can reduce the gate complexity to $O(n^4)$. Here we introduce a new VQE ansatz based on the particle preserving exchange gate [20, 25] to achieve qubit excitations, which has gate complexity up-bounded to $O(n^4)$ and has comparable accuracy compared to first order trotterization UCCSD VQE. By reducing the gate complexity, QCCSD VQE ansatz—qubit coupled cluster singles and doubles (QCCSD) VQE ansatz, might be more favorable for current NISQ devices.

The rest of the paper is organized as follows: the first section gives a brief introduction to the method of UCCSD VQE ansatz. Then we give a detailed description of QCCSD VQE ansatz. We also show QCCSD VQE is a simplified version of the first order trotterization UCCSD VQE. Finally, we give the numerical simulation results of BeH_2, H_2O, N_2, H_4 and H_6 using first order trotterization UCCSD VQE and QCCSD VQE ansatz.

2. UCCSD VQE

The electronic structure Hamiltonian can be written in second quantization as:

$$H = h_0 + \sum_{ij} h_{ij} a_i^\dagger a_j + \frac{1}{2} \sum_{ijkl} h_{ijkl} a_i^\dagger a_j^\dagger a_k a_l \tag{1}$$

where h_0 is the nuclear repulsion energy, the one-electron integrals h_{ij} and the two-electron integrals h_{ijkl} can be calculated by orbital integrals. Using Jordan–Wigner transformation we can rewrite the Hamiltonian in the Pauli matrices form:

$$H = \sum_{i,\alpha} a_\alpha^i \sigma_\alpha^i + \sum_{ij,\alpha\beta} b_{\alpha\beta}^{ij} \sigma_\alpha^i \sigma_\beta^j + \cdots \tag{2}$$

where $a_\alpha^i, b_{\alpha\beta}^{ij}$ are general coefficients and $\sigma_\alpha^i \sigma_\beta^j$ are Pauli matrices σ_x, σ_y, σ_z and 2×2 identity matrix.

In unitary coupled clustered single double excitations, we can calculate the ground state from the Hartree–Fock reference state by excitation operators of the form:

$$|\phi\rangle = e^{T(\vec{\theta}) - T^\dagger(\vec{\theta})} |\phi_{HF}\rangle \tag{3}$$

where $T(\vec{\theta}) = T_1(\vec{\theta}_1) + T_2(\vec{\theta}_2)$ is the excitation operator, $|\phi_{HF}\rangle$ is the Hartree–Fock reference state and $\vec{\theta}$ is the set of adjustable parameters. The single excitation operator can be written as $T_1(\vec{\theta}_1) = \sum_{i,j} \theta_{ij} a_i^\dagger a_j$ and the double excitation operator can be written as $T_2(\vec{\theta}_2) = \sum_{i,j,k,l} \theta_{ijkl} a_i^\dagger a_j^\dagger a_k a_l$. We can minimize $\langle \phi | H | \phi \rangle$ to get the ground state energy by optimizing $\vec{\theta}$.

Considering an n qubits Hamiltonian, the number of spin orbitals is n and the total number of excitation terms in T is $O(\binom{N_{occ}}{2} \times \binom{N_{virt}}{2})$, where N_{occ} is the number of occupied spin orbitals, N_{virt} is the number of virtual spin orbitals. $n = N_{occ} + N_{virt}$ is the number of qubits of the Hamiltonian or the total number of spin orbitals.

The first order trotterization UCCSD operator can be written as:

$$e^{T(\vec{\theta}) - T^\dagger(\vec{\theta})} \approx \prod_{i,j} e^{\theta_{ij}(a_i^\dagger a_j - a_j^\dagger a_i)} \times \prod_{i,j,k,l} e^{\theta_{ijkl}(a_i^\dagger a_j^\dagger a_k a_l - a_l^\dagger a_k^\dagger a_j a_i)}. \tag{4}$$

To map the first order trotterization UCCSD to quantum computer, we use same transformation, Jordan–Wigner transformation, as we do for the Hamiltonian to transform creation and annihilation operators into Pauli matrices. Each term in equation (4) can be implemented as unitary quantum gates by Jordan–Wigner transformation. Since the cost of Jordan–Wigner transformation for each term is $O(n)$ [1], the gate complexity for the first order trotterization UCCSD VQE is $O(\binom{N_{occ}}{2} \times \binom{N_{virt}}{2} \times n) < O(n^5)$ using Jordan–Wigner transformation [1, 19].

UCCSD VQE has shown high accuracy in electronic structure calculations [1, 19, 21, 22]. However, one problem of the UCCSD VQE is the large complexity. The first order trotterization UCCSD VQE has up-bounded $O(n^4)$ terms and $O(n^5)$ gate complexity using Jordan–Wigner transformation. Here, we propose a new qubit coupled cluster singles and doubles VQE ansatz using the particle preserving exchange gate [20, 25]. The gate complexity of QCCSD ansatz scales as $O(\binom{N_{occ}}{2} \times \binom{N_{virt}}{2}) < O(n^4)$. In the numerical simulations, we show that QCCSD ansatz can achieve comparable accuracy to the first order trotterization UCCSD VQE.

3. QCCSD VQE ansatz

After Jordan–Winger transformation, each qubit represents whether the corresponding spin orbital is occupied or not. When qubit i is in $|0\rangle$, spin orbital i is not occupied and when qubit i is in $|1\rangle$ spin orbital i

$$U'_{ex}(\theta) = \begin{bmatrix} 1 & 0 & 0 & 0 & 0 & 0 & 0 & 0 & 0 & 0 & 0 & 0 & 0 & 0 & 0 & 0 \\ 0 & 1 & 0 & 0 & 0 & 0 & 0 & 0 & 0 & 0 & 0 & 0 & 0 & 0 & 0 & 0 \\ 0 & 0 & 1 & 0 & 0 & 0 & 0 & 0 & 0 & 0 & 0 & 0 & 0 & 0 & 0 & 0 \\ 0 & 0 & 0 & 1 & 0 & 0 & 0 & 0 & 0 & 0 & 0 & 0 & 0 & 0 & 0 & 0 \\ 0 & 0 & 0 & 0 & 1 & 0 & 0 & 0 & 0 & 0 & 0 & 0 & 0 & 0 & 0 & 0 \\ 0 & 0 & 0 & 0 & 0 & cos\theta & 0 & 0 & 0 & 0 & -sin\theta & 0 & 0 & 0 & 0 & 0 \\ 0 & 0 & 0 & 0 & 0 & 0 & 1 & 0 & 0 & 0 & 0 & 0 & 0 & 0 & 0 & 0 \\ 0 & 0 & 0 & 0 & 0 & 0 & 0 & 1 & 0 & 0 & 0 & 0 & 0 & 0 & 0 & 0 \\ 0 & 0 & 0 & 0 & 0 & 0 & 0 & 0 & 1 & 0 & 0 & 0 & 0 & 0 & 0 & 0 \\ 0 & 0 & 0 & 0 & 0 & 0 & 0 & 0 & 0 & 1 & 0 & 0 & 0 & 0 & 0 & 0 \\ 0 & 0 & 0 & 0 & 0 & sin\theta & 0 & 0 & 0 & 0 & cos\theta & 0 & 0 & 0 & 0 & 0 \\ 0 & 0 & 0 & 0 & 0 & 0 & 0 & 0 & 0 & 0 & 0 & 1 & 0 & 0 & 0 & 0 \\ 0 & 0 & 0 & 0 & 0 & 0 & 0 & 0 & 0 & 0 & 0 & 0 & 1 & 0 & 0 & 0 \\ 0 & 0 & 0 & 0 & 0 & 0 & 0 & 0 & 0 & 0 & 0 & 0 & 0 & 1 & 0 & 0 \\ 0 & 0 & 0 & 0 & 0 & 0 & 0 & 0 & 0 & 0 & 0 & 0 & 0 & 0 & 1 & 0 \\ 0 & 0 & 0 & 0 & 0 & 0 & 0 & 0 & 0 & 0 & 0 & 0 & 0 & 0 & 0 & 1 \end{bmatrix}$$

Figure 1. Matrix of $U'_{ex}(\theta)$.

is occupied. Thus we can write down a particle preserving exchange gate U_{ex} [20, 25] between two qubits as:

$$U_{ex}(\theta) = \begin{bmatrix} 1 & 0 & 0 & 0 \\ 0 & \cos\theta & -\sin\theta & 0 \\ 0 & \sin\theta & \cos\theta & 0 \\ 0 & 0 & 0 & 1 \end{bmatrix}.$$

The particle preserving exchange gate U_{ex} will not change the total number occupation when applied to arbitrary states. Suppose we have two qubits in $|10\rangle$, which represents that the first spin orbital is occupied and the second spin orbital is not occupied. If we apply U_{ex} to this state we have:

$$U_{ex}(\theta)|10\rangle = \cos\theta|10\rangle - \sin\theta|01\rangle \tag{5}$$

which corresponds to a single excitation between one spin occupied and one virtual spin orbitals.

We can also write down a particle preserving exchange gate U'_{ex} between four qubits as in figure 1. Suppose we have four qubits in $|1010\rangle$, which represents the first and the third spin orbitals are occupied while the second and the fourth spin orbitals are not occupied. If we apply U'_{ex} to this state we have:

$$U'_{ex}(\theta)|1010\rangle = \cos\theta|1010\rangle - \sin\theta|0101\rangle \tag{6}$$

which corresponds to a double excitation between two occupied and two virtual spin orbitals.

We can write down an operator U by U_{ex} and U'_{ex} to achieve single and double excitations from the Hartree–Fock reference state:

$$|\Phi\rangle = U(\vec{\Theta})|\phi_{HF}\rangle = \prod_{i,j} U_{ex,i,j}(\theta_{ij}) \prod_{i,j,k,l} U'_{ex,i,j,k,l}(\theta_{ijkl})|\phi_{HF}\rangle \tag{7}$$

$U_{ex,i,j}$ represents U_{ex} between qubits $i\,j$ where qubit i represents the occupied orbital and qubit j represents the virtual orbital. $U'_{ex,i,j,k,l}$ represents U'_{ex} between qubits $i\,j\,k\,l$ where qubit i, k represent occupied orbitals and qubit j, l represent the virtual orbitals. $\vec{\Theta}$ is the set of adjustable parameters. We can minimize $\langle\Phi|H|\Phi\rangle$ to get the ground state energy by optimizing $\vec{\Theta}$.

$U_{ex}(\theta)$ and $U'_{ex}(\theta)$ can be decomposed into elementary quantum gates with gate complexity $O(1)$ because the sizes of matrices of $U_{ex}(\theta)$ and $U'_{ex}(\theta)$ are $O(1)$. A possible decomposition of $U_{ex}(\theta)$ is by Gray code [26]:
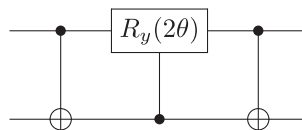
A possible decomposition of $U'_{ex}(\theta)$ following [27] is shown in figure 2. A number of groups have shown how to reduce the gate complexity of coupled cluster methods [28–30] on quantum computer and may be able to be applied to QCCSD VQE. Recently, O'Gorman *et al* [31] show that by using fermionic swap networks one can reduce the circuit depth to $O(n^{k-1})$ when implementing set of k qubits gates on n logical qubits, which may reduce the depth of QCCSD VQE by a factor of n. This is a possible future improvement but out of the scope of this paper. Recently, Yordanov and Barnes [27] proposed a new decomposition of

Figure 2. Decomposition of $U'_{\mathrm{ex}}(\theta)$ follows [27].
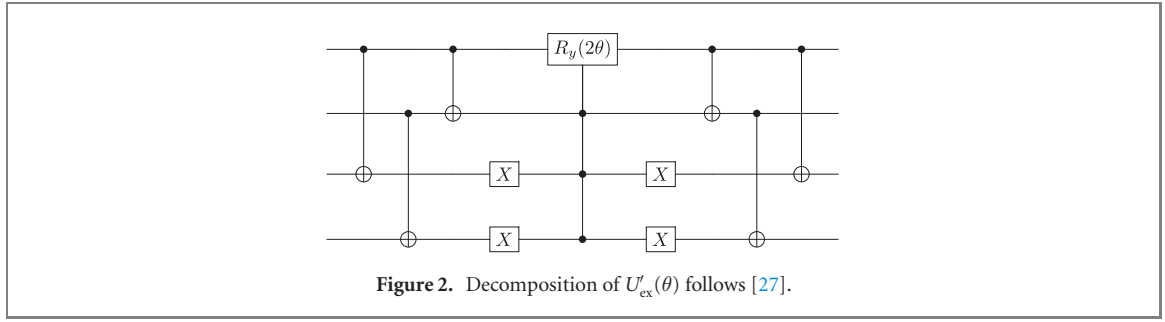
UCCSD VQE into two steps: first applying the qubit excitation gates, which are the particle preserving exchange gates in our QCCSD VQE used for single and double excitations though termed differently, then applying CNOT gates to include the parity information. In our simulation, $U_{\mathrm{ex}}(\theta)$ and $U'_{\mathrm{ex}}(\theta)$ are implemented as single unitary gates in Qiskit [32].

3.1. Excitation list selection

One important part of the proposed VQE is to choose the excitation list, or to decide between which spin orbitals the excitation will occur. Spin preserving VQE ansatzes, which preserve the net spin magnetization s_z, have been widely studied [33, 34]. We use the same strategy and choose the excitation list only allowing spin preserving excitations. More details can be found in the appendix . The term complexity of our ansatz scales as $O(\binom{N_{\mathrm{occ}}}{2} \times \binom{N_{\mathrm{virt}}}{2})$. The required elementary quantum gates for U_{ex} and U'_{ex} are both $O(1)$. Thus the gate complexity of our ansatz scales as $O(\binom{N_{\mathrm{occ}}}{2} \times \binom{N_{\mathrm{virt}}}{2}) < O(n^4)$. One should note that, for linear connectivity, if no extra strategies are applied, the straightforward compilation will make the complexity of proposed QCCSD VQE scale up to $O(n^5)$. However, this complexity can be reduced by applying strategies for the compilation as done for example in the generalized swap network [31]. Moreover, a recent study [33] shows that considering the total spin s preserving may also help to achieve better accuracy, QCCSD VQE ansatz may also be able to be modified to preserve the total spin s, which will be done in the future work.

3.2. Relation to UCCSD VQE ansatz

Here, we present that QCCSD VQE ansatz is a simplified version of UCCSD VQE ansatz. Consider a single excitation term in first order trotterization UCCSD VQE:

$$e^{\theta(a_i^\dagger a_j - a_j^\dagger a_i)}. \tag{8}$$

Without loss of generality, we can require $i \in virt$ and $j \in occ$ where *virt* represents virtual orbitals and *occ* represents occupied orbitals. Furthermore we can set $i > j$ and if using Jordan–Wigner transformation we get:

$$e^{\frac{i\theta}{2}\sigma_y^j\sigma_x^i \otimes_{a=j+1}^{i-1}\sigma_z^a} e^{\frac{-i\theta}{2}\sigma_x^j\sigma_y^i \otimes_{a=j+1}^{i-1}\sigma_z^a}. \tag{9}$$

In equation (9), $\otimes_{a=j+1}^{i-1}\sigma_z^a$ counts for the parity of qubits from $j+1$ to $i-1$. If we remove the parity term we get:

$$e^{\frac{i\theta}{2}\sigma_y^j\sigma_x^i} e^{\frac{-i\theta}{2}\sigma_x^j\sigma_y^i} = U_{\mathrm{ex},j,i}(-\theta). \tag{10}$$

Thus our particle conservation exchange gate $U_{\mathrm{ex},j,i}$ counts for the single excitation term of qubits $j\,i$ in first order trotterization UCCSD VQE without considering the parity of qubits from $j+1$ to $i-1$. Also, consider a double excitation term in first order trotterization UCCSD VQE:

$$e^{\theta(a_i^\dagger a_j^\dagger a_k a_l - a_l^\dagger a_k^\dagger a_j a_i)} \tag{11}$$

Without loss of generality, we can require $i < j \in virt$ and $l < k \in occ$. Furthermore we can choose the order $j > k > i > l$ and if using Jordan–Wigner transformation we get:

$$e^{\frac{-i\theta}{8}\sigma_x^l\sigma_x^i\sigma_x^k\sigma_y^j \otimes_{a=l+1}^{i-1}\sigma_z^a \otimes_{a=k+1}^{j-1}\sigma_z^a} e^{\frac{-i\theta}{8}\sigma_x^l\sigma_y^i\sigma_x^k\sigma_x^j \otimes_{a=l+1}^{i-1}\sigma_z^a \otimes_{a=k+1}^{j-1}\sigma_z^a}$$

$$e^{\frac{-i\theta}{8}\sigma_x^l\sigma_y^i\sigma_y^k\sigma_y^j \otimes_{a=l+1}^{i-1}\sigma_z^a \otimes_{a=k+1}^{j-1}\sigma_z^a} e^{\frac{-i\theta}{8}\sigma_y^l\sigma_y^i\sigma_x^k\sigma_y^j \otimes_{a=l+1}^{i-1}\sigma_z^a \otimes_{a=k+1}^{j-1}\sigma_z^a}$$

$$e^{\frac{-i\theta}{8}\sigma_x^l\sigma_x^i\sigma_y^k\sigma_x^j \otimes_{a=l+1}^{i-1}\sigma_z^a \otimes_{a=k+1}^{j-1}\sigma_z^a} e^{\frac{-i\theta}{8}\sigma_y^l\sigma_x^i\sigma_x^k\sigma_x^j \otimes_{a=l+1}^{i-1}\sigma_z^a \otimes_{a=k+1}^{j-1}\sigma_z^a} \tag{12}$$

$$e^{\frac{-i\theta}{8}\sigma_y^l\sigma_x^i\sigma_y^k\sigma_y^j \otimes_{a=l+1}^{i-1}\sigma_z^a \otimes_{a=k+1}^{j-1}\sigma_z^a} e^{\frac{-i\theta}{8}\sigma_y^l\sigma_y^i\sigma_y^k\sigma_x^j \otimes_{a=l+1}^{i-1}\sigma_z^a \otimes_{a=k+1}^{j-1}\sigma_z^a}.$$

In equation (12) $\otimes_{a=l+1}^{i-1}\sigma_z^a \otimes_{a=k+1}^{j-1}\sigma_z^a$ counts for the parity of qubits from $l+1$ to $i-1$ and from $k+1$ to $j-1$. If we remove the parity term we get:

$$e^{\frac{-i\theta}{8}\sigma_x^l\sigma_x^i\sigma_x^k\sigma_y^j}e^{\frac{-i\theta}{8}\sigma_x^l\sigma_y^i\sigma_x^k\sigma_x^j}e^{\frac{-i\theta}{8}\sigma_x^l\sigma_y^i\sigma_y^k\sigma_y^j}e^{\frac{-i\theta}{8}\sigma_y^l\sigma_y^i\sigma_x^k\sigma_y^j}$$

$$e^{\frac{i\theta}{8}\sigma_x^l\sigma_x^i\sigma_y^k\sigma_x^j}e^{\frac{i\theta}{8}\sigma_y^l\sigma_x^i\sigma_x^k\sigma_x^j}e^{\frac{i\theta}{8}\sigma_y^l\sigma_x^i\sigma_y^k\sigma_y^j}e^{\frac{i\theta}{8}\sigma_y^l\sigma_y^i\sigma_y^k\sigma_x^j} = U'_{\mathrm{ex},l,i,k,j}(-\theta). \tag{13}$$

Thus our particle preserving exchange gate $U'_{\mathrm{ex},l,i,k,j}$ counts for the double excitation term of qubits l,k,i,j in first order trotterization UCCSD VQE without considering the parity of qubits from $l+1$ to $i-1$ and from $k+1$ to $j-1$. One should be aware that if different order of spin orbitals is used, the double excitation term with parity terms removed may equal to $U'_{\mathrm{ex}}(\theta)$. QCCSD VQE is the simplified version of first order trotterization UCCSD VQE. The reduced gate complexity of our VQE comes from removing the parity term in UCCSD VQE. Recently Smart *et al* [35] presented an efficient ansatz for two-electron system, showing that fermionic double excitations can be simplified to qubit double excitations in the two-electron system, which indicates the QCCSD VQE has the same double excitation terms as the UCCSD VQE for a two-electron system.

4. Numerical simulation results

In this section, we present numerical results of BeH_2, H_2O, N_2, H_4 and H_6 by using QCCSD VQE with gates U_{ex} and U'_{ex}. To compare performance of QCCSD VQE, we also present the results by using first order trotterization UCCSD VQE implemented by Qiskit [32]. For each numerical simulation, the orbital integrals are calculated using STO-3G minimal basis by PySCF [36] and the Hamiltonian is obtained by Jordan–Wigner transformation. The optimization is performed by the sequential least squares programming algorithm [37]. The input state is the Hartree–Fock reference state and all parameters are initialized as 0 for both ansatzes. The bounds for all parameters for both ansatzes are set to $[-\pi, \pi]$. The energy thresholds for convergence is set to 10^{-6} Hartree with maximum 500 iterations. The noiseless simulation is done by Qiskit [32] with version 0.14.1. In the figures in this section, QCCSD VQE represent the proposed qubit coupled cluster singles and doubles VQE ansatz while UCCSD VQE represents the first order trotterization UCCSD VQE ansatz implemented by Qiskit [32].

Complete active space approach [38], which divides the space to active orbitals and inactive orbitals, has been applied to reduce the qubits of molecule Hamiltonian in quantum simulation. To investigate the effect of the size of active space, we compare the performance of QCCSD ansatz for different sizes of active spaces for the same molecule.

For BeH_2 we choose three different active spaces: first 2 spin orbitals with lowest energies are always filled and first 2 spin orbitals with highest energies are always empty, corresponding to 10 active spin orbitals with 4 electrons or 10 qubits Hamiltonian. First 2 spin orbitals with lowest energies are always filled, corresponding to 12 active spin orbitals with 4 electrons or 12 qubits Hamiltonian. No spin orbitals are always filled or always empty, corresponding to 14 active spin orbitals with 6 electrons or 14 qubits Hamiltonian. We compare the errors between the ground state energies from the VQE results and the ground state energies from the diagonalization of the corresponding Hamiltonian as in figure 3. We can see that, although the size of the active space is increased, our QCCSD VQE achieves similar accuracy as the first order trotterization UCCSD VQE.

For H_2O we choose three different active spaces: first 4 spin orbitals with lowest energies are always filled, corresponding to 10 active spin orbitals with 6 electrons or 10 qubits Hamiltonian; first 2 spin orbitals with lowest energies are always filled, corresponding to 12 active spin orbitals with 8 electrons or 12 qubits Hamiltonian and no spin orbitals are always filled or always empty, corresponding to 14 active spin orbitals with 10 electrons or 14 qubits Hamiltonian. We compare the errors between the ground state energies from the VQE results and the ground state energies from the diagonalization of the corresponding Hamiltonian as in figure 4 for different Hamiltonian. For 10 qubits H_2O Hamiltonian our QCCSD VQE achieves almost the same accuracy as the first order trotterization UCCSD VQE except at one point. For 12 and 14 qubits H_2O Hamiltonian, with increased size of active space, our QCCSD VQE performs a little worse compared to the first order trotterization UCCSD VQE the error increased from 10^{-5} to 10^{-3} Hartree, but the error is still within or around the chemical accuracy.

For N_2 we choose four different active spaces: first 8 spin orbitals with lowest energies are always filled and first 2 spin orbitals with highest energies are always empty, corresponding to 10 active spin orbitals with 6 electrons or 10 qubits Hamiltonian; first 8 spin orbitals with lowest energies are always filled, corresponding to 12 active spin orbitals with 6 electrons or 12 qubits Hamiltonian; first 6 spin orbitals with lowest energies are always filled, corresponding to 14 active spin orbitals with 8 electrons or 14 qubits
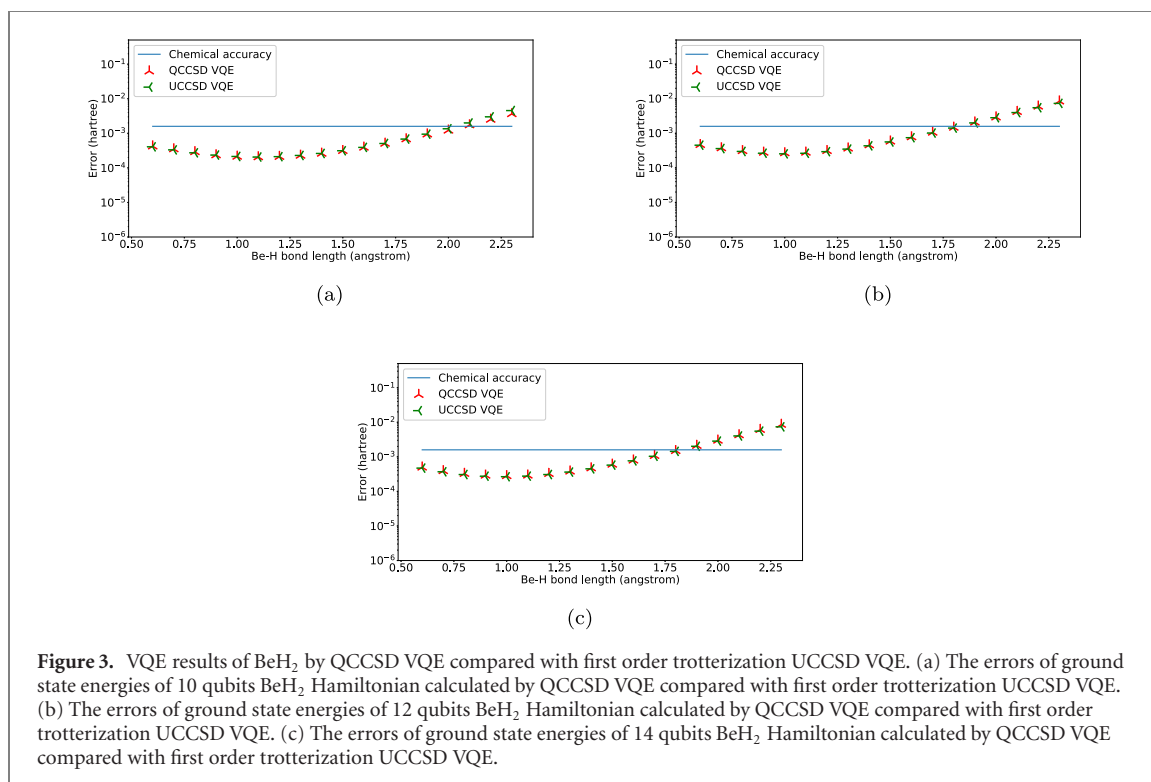
Figure 3. VQE results of BeH$_2$ by QCCSD VQE compared with first order trotterization UCCSD VQE. (a) The errors of ground state energies of 10 qubits BeH$_2$ Hamiltonian calculated by QCCSD VQE compared with first order trotterization UCCSD VQE. (b) The errors of ground state energies of 12 qubits BeH$_2$ Hamiltonian calculated by QCCSD VQE compared with first order trotterization UCCSD VQE. (c) The errors of ground state energies of 14 qubits BeH$_2$ Hamiltonian calculated by QCCSD VQE compared with first order trotterization UCCSD VQE.

Figure 4. VQE results of H$_2$O by QCCSD VQE compared with first order trotterization UCCSD VQE. (a) The errors of ground state energies of 10 qubits H$_2$O Hamiltonian calculated by QCCSD VQE compared with first order trotterization UCCSD VQE. (b) The errors of ground state energies of 12 qubits H$_2$O Hamiltonian calculated by QCCSD VQE compared with first order trotterization UCCSD VQE. (c) The errors of ground state energies of 14 qubits H$_2$O Hamiltonian calculated by QCCSD VQE compared with first order trotterization UCCSD VQE.
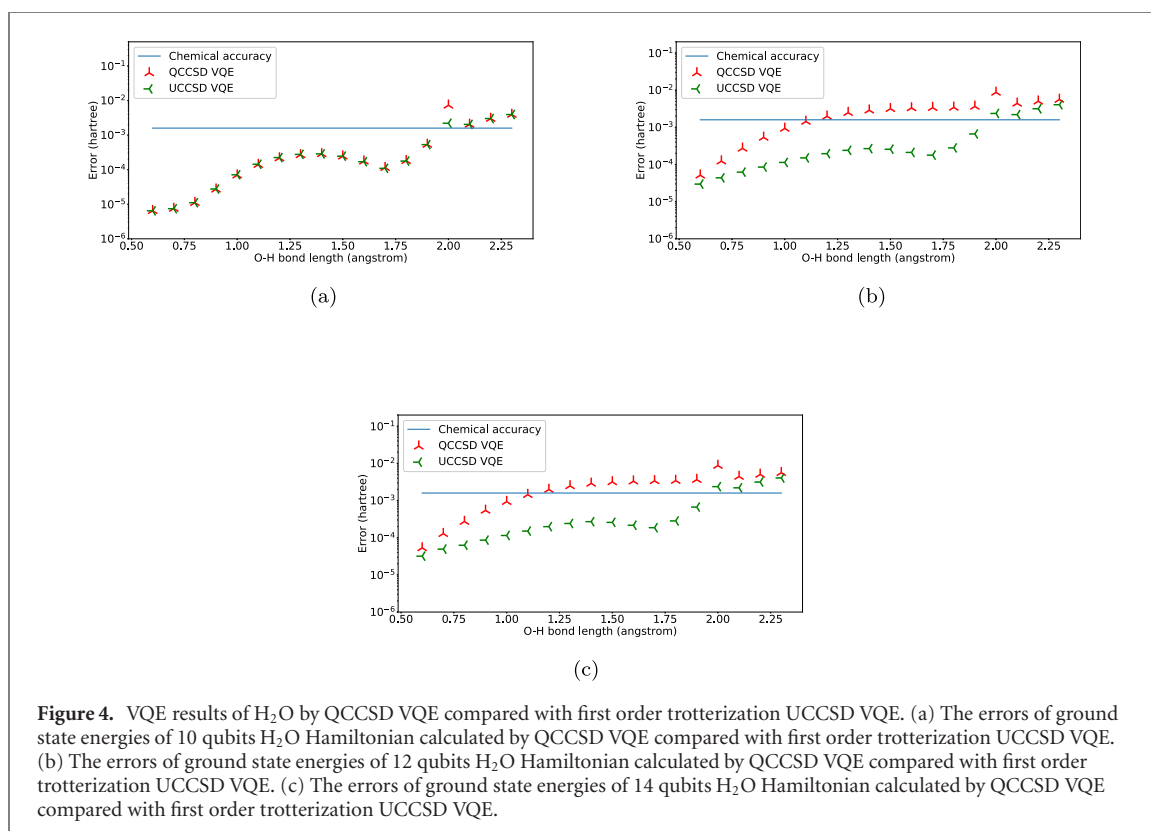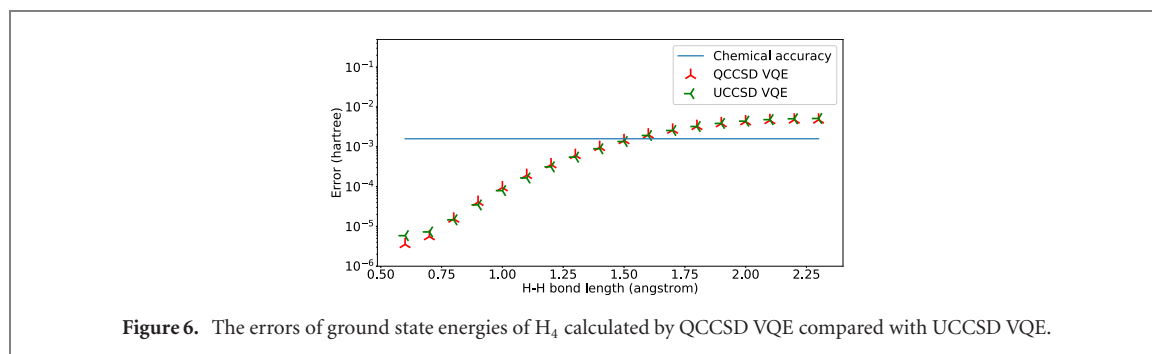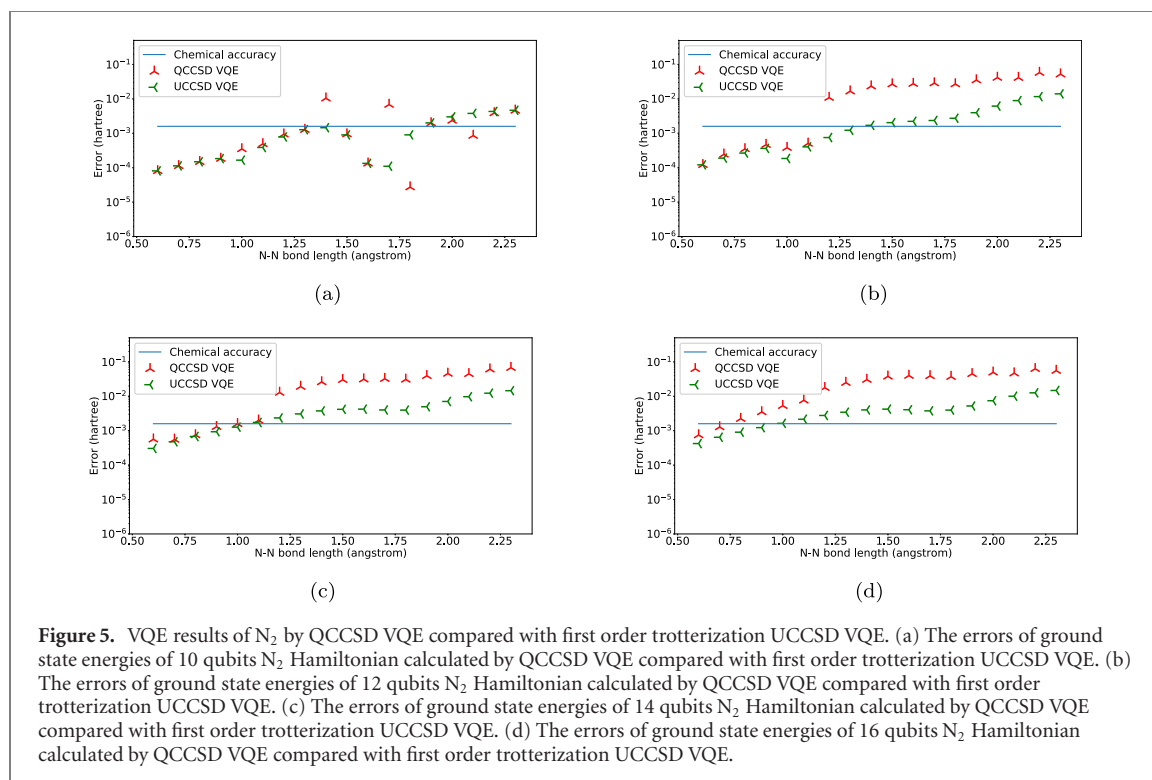
Hamiltonian. First 4 spin orbitals with lowest energies are always filled, corresponding to 16 active spin orbitals with 10 electrons or 16 qubits Hamiltonian. We compare the errors between the ground state energies from the VQE results and the ground state energies from the diagonalization of the corresponding Hamiltonian as in figure 5 for different Hamiltonian. For 10 qubits N$_2$ Hamiltonian our QCCSD VQE achieves almost same or even better accuracy as the first order trotterization UCCSD VQE except one point. For 12, 14 and 16 qubits N$_2$ Hamiltonian, with increased size of active space, our QCCSD VQE performs

Figure 5. VQE results of N_2 by QCCSD VQE compared with first order trotterization UCCSD VQE. (a) The errors of ground state energies of 10 qubits N_2 Hamiltonian calculated by QCCSD VQE compared with first order trotterization UCCSD VQE. (b) The errors of ground state energies of 12 qubits N_2 Hamiltonian calculated by QCCSD VQE compared with first order trotterization UCCSD VQE. (c) The errors of ground state energies of 14 qubits N_2 Hamiltonian calculated by QCCSD VQE compared with first order trotterization UCCSD VQE. (d) The errors of ground state energies of 16 qubits N_2 Hamiltonian calculated by QCCSD VQE compared with first order trotterization UCCSD VQE.

Figure 6. The errors of ground state energies of H_4 calculated by QCCSD VQE compared with UCCSD VQE.

worse compared to the first order trotterization UCCSD VQE. This indicates that the removal of parity terms in excitation operators may affect accuracy of the the couple cluster method for larger system size.

For H_4 chain we do not have any restrictions on the spin orbitals, corresponding to 8 active spin orbitals and 4 active electrons. We also show the error between the ground state energies from VQE results and the ground state energies from the diagonalization of the corresponding Hamiltonian as in figure 6. Our QCCSD VQE achieves the same level accuracy compared to the first order trotterization UCCSD VQE.

For H_6 chain we do not have any restrictions on the spin orbitals, corresponding to 12 active spin orbitals and 6 active electrons. We also show the error between the ground state energies from VQE results and the ground state energies from the diagonalization of the corresponding Hamiltonian as in figure 7. Our QCCSD VQE achieves same level accuracy compared to the first order trotterization UCCSD VQE.

5. Discussion and conclusion

In simulations, we have shown that increasing the size of active space will have little effect on the accuracy of the QCCSD VQE for BeH_2. Our QCCSD VQE can still achieve good results for larger active space for H_2O but performs worse than UCCSD VQE for N_2. Here we present the overlap $|\langle \phi_{HF} | \phi_{ground} \rangle|^2$ where $|\phi_{HF}\rangle$ is the input Hartree–Fock state and $|\phi_{ground}\rangle$ is the exact ground state obtained by diagonalization of
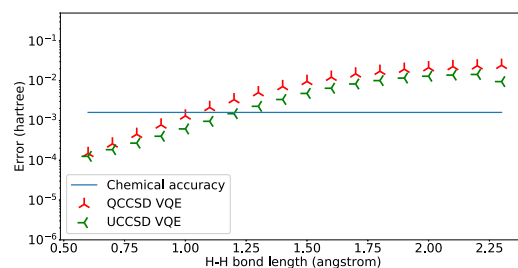
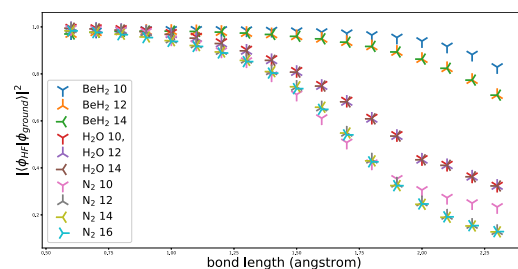**Figure 7.** The errors of ground state energies of H_6 calculated by QCCSD VQE compared with UCCSD VQE.

Figure 8. The overlap $|\langle\phi_{HF}|\phi_{ground}\rangle|^2$ where $|\phi_{HF}\rangle$ is the input Hartree–Fock state and $|\phi_{ground}\rangle$ is the exact ground state obtained by diagonalization of the corresponding Hamiltonian for BeH_2, H_2O and N_2 of different active spaces. BeH_2 10 represents the BeH_2 10 qubits Hamiltonian. BeH_2 12 represents the BeH_2 12 qubits Hamiltonian. BeH_2 14 represents the BeH_2 14 qubits Hamiltonian. H_2O 10 represents the H_2O 10 qubits Hamiltonian. H_2O 12 represents the H_2O 12 qubits Hamiltonian. H_2O 14 represents the H_2O 14 qubits Hamiltonian. N_2 10 represents the N_2 10 qubits Hamiltonian. N_2 12 represents the N_2 12 qubits Hamiltonian. N_2 14 represents the N_2 14 qubits Hamiltonian. N_2 16 represents the N_2 16 qubits Hamiltonian.

the corresponding Hamiltonian for BeH_2, H_2O and N_2 of different active spaces. in figure 8. We can see that the overlaps for BeH_2 with different sizes of active space are large, which may indicate very few excitation operators and small amplitudes of excitation operators (θ in equation (4)) are needed to approximate the exact ground state and removal of parity terms will have little effect on results. However, for N_2, the overlap for N_2 is small when the size of active space increases and bond length is large, which may indicate that a large portion of excitation operators and large amplitudes of excitation operators (θ in equation (4)) are needed to approximate the exact ground state, thus removal of parity terms may have some effects on results.

In conclusion, we have introduced a new VQE ansatz based on the particle preserving exchange gate [20, 25]. We have shown QCCSD VQE has reduced gate complexity from up-bounded to $O(n^5)$ of UCCSD VQE to up-bounded to $O(n^4)$ if using Jordan–Wigner transformation. In numerical simulations of BeH_2, H_2O, N_2, H_4 and H_6, we have shown that QCCSD VQE have achieved comparable accuracy compared to UCCSD VQE. With reduced complexity and high accuracy, QCCSD VQE ansatz might provide a new promising direction to implement electronic structure calculations on NISQ devices with chemical accuracy.

Acknowledgment

Appendix

As shown in [22], the ordering of excitation operators in the Trotterized UCCSD VQE may have impact on the final results. To eliminate the effect of the operator ordering, we choose the same ordering as in the implementation of first order trotterization UCCSD VQE in Qiskit [32]. The ordering is also presented in the below algorithm 1.

Algorithm 1. Qubit coupled cluster singles and doubles VQE considering spin preserving.

1: **for** orbital$_i$ in spin-up occupied orbitals **do**
2:    **for** orbital$_j$ in spin-up virtual orbitals **do**
3:       Construct U_{ex} between qubit i and j.
4:    **end for**
5: **end for**
6: **for** orbital$_k$ in spin-down occupied orbitals **do**
7:    **for** orbital$_l$ in spin-down virtual orbitals **do**
8:       Construct U_{ex} between qubit k and l.
9:    **end for**
10: **end for**
11: **for** orbital$_i$ in spin-up occupied orbitals **do**
12:    **for** orbital$_j$ in spin-up virtual orbitals **do**
13:       **for** orbital$_k$ in spin-down occupied orbitals **do**
14:          **for** orbital$_l$ in spin-down virtual orbitals **do**
15:             Construct U'_{ex} between qubit $i\,j\,k$ and l.
16:          **end for**
17:       **end for**
18:    **end for**
19: **end for**
20: **for** orbital$_i$ in spin-up occupied orbitals **do**
21:    **for** orbital$_k$ in spin-up virtual orbitals **do**
22:       **for** orbital$_j$ ($j > i$) in spin-up occupied orbitals **do**
23:          **for** orbital$_l$ ($l > k$) in spin-up virtual orbitals **do**
24:             Construct U'_{ex} between qubit $i\,k\,j$ and l.
25:          **end for**
26:       **end for**
27:    **end for**
28: **end for**
29: **for** orbital$_i$ in spin-down occupied orbitals **do**
30:    **for** orbital$_k$ in spin-down virtual orbitals **do**
31:       **for** orbital$_j$ ($j > i$) in spin-down occupied orbitals **do**
32:          **for** orbital$_l$ ($l > k$) in spin-down virtual orbitals **do**
33:             Construct U'_{ex} between qubit $i\,k\,j$ and l.
34:          **end for**
35:       **end for**
36:    **end for**
37: **end for**

ORCID iDs

Rongxin Xia ⬡ https://orcid.org/0000-0003-3536-1140
Sabre Kais ⬡ https://orcid.org/0000-0003-0574-5346

References

[1] Cao Y *et al* 2019 Quantum chemistry in the age of quantum computing *Chem. Rev.* **119** 10856–915
[2] Kitaev A Y 1995 Quantum measurements and the abelian stabilizer problem arXiv:quant-ph/9511026
[3] Abrams D S and Lloyd S 1997 Simulation of many-body fermi systems on a universal quantum computer *Phys. Rev. Lett.* **79** 2586
[4] Aspuru-Guzik A, Dutoi A D, Love P J and Head-Gordon M 2005 Simulated quantum computation of molecular energies *Science* **309** 1704–7
[5] Wang H, Kais S, Aspuru-Guzik A and Hoffmann M R 2008 Quantum algorithm for obtaining the energy spectrum of molecular systems *Phys. Chem. Chem. Phys.* **10** 5388–93
[6] Daskin A and Kais S 2011 Decomposition of unitary matrices for finding quantum circuits: application to molecular Hamiltonians *J. Chem. Phys.* **134** 144112
[7] Daskin A, Grama A, Kollias G and Kais S 2012 Universal programmable quantum circuit schemes to emulate an operator *J. Chem. Phys.* **137** 234112
[8] Kais S 2014 *Advances in Chemical Physics, Quantum Information and Computation for Chemistry* vol 154 (New York: Wiley)
[9] Bian T, Murphy D, Xia R, Ammar D and Kais S 2019 Quantum computing methods for electronic states of the water molecule *Mol. Phys.* **117** 2069–82
[10] Alberto P, McClean J, Shadbolt P, Yung M-H, Zhou X-Q, Love P J, Aspuru-Guzik A and O'brien J L 2014 A variational eigenvalue solver on a photonic quantum processor *Nat. Commun.* **5** 4213
[11] Yung M-H, Casanova J, Mezzacapo A, Mcclean J, Lamata L, Aspuru-Guzik A and Solano E 2014 From transistor to trapped-ion computers for quantum chemistry *Sci. Rep.* **4** 3589
[12] Barends R *et al* 2015 Digital quantum simulation of fermionic models with a superconducting circuit *Nat. Commun.* **6** 1–7
[13] McClean J R, Romero J, Babbush R and Aspuru-Guzik A 2016 The theory of variational hybrid quantum-classical algorithms *New J. Phys.* **18** 023023
[14] Xia R and Kais S 2018 Quantum machine learning for electronic structure calculations *Nat. Commun.* **9** 1–6
[15] Preskill J 2018 Quantum computing in the NISQ era and beyond *Quantum* **2** 79
[16] O'Malley P J J *et al* 2016 Scalable quantum simulation of molecular energies *Phys. Rev.* X **6** 031007

[17] Kandala A, Mezzacapo A, Temme K, Takita M, Brink M, Chow J M and Gambetta J M 2017 Hardware-efficient variational quantum eigensolver for small molecules and quantum magnets *Nature* **549** 242–6

[18] Bartlett R J and Musiał M 2007 Coupled-cluster theory in quantum chemistry *Rev. Mod. Phys.* **79** 291

[19] Romero J, Babbush R, McClean J R, Hempel C, Love P J and Aspuru-Guzik A 2018 Strategies for quantum computing molecular energies using the unitary coupled cluster ansatz *Quantum Sci. Technol.* **4** 014008

[20] Barkoutsos P K *et al* 2018 Quantum algorithms for electronic structure calculations: particle–hole Hamiltonian and optimized wave-function expansions *Phys. Rev.* A **98** 022322

[21] Shen Y, Zhang X, Zhang S, Zhang J-N, Yung M-H and Kim K 2017 Quantum implementation of the unitary coupled cluster for simulating molecular electronic structure *Phys. Rev.* A **95** 020501

[22] Grimsley H R, Claudino D, Economou S E, Barnes E and Mayhall N J 2019 Is the trotterized UCCSD ansatz chemically well-defined? *J. Chem. Theory Comput.* **16** 1–6

[23] Poulin D, Hastings M B, Wecker D, Wiebe N, Doberty A C and Troyer M 2015 The trotter step size required for accurate quantum simulation of quantum chemistry *Quantum Information & Computation* vol 15 (Princeton, NJ: Rinton Press) pp 361–84

[24] Motta M, Ye E, McClean J R, Li Z, Minnich A J, Babbush R and Chan G K 2018 Low rank representations for quantum simulation of electronic structure arXiv:1808.02625

[25] McKay D C, Filipp S, Mezzacapo A, Magesan E, Chow J M and Gambetta J M 2016 Universal gate for fixed-frequency qubits via a tunable bus *Phys. Rev. Appl.* **6** 064007

[26] Nielsen M A and Chuang I 2002 *Quantum Computation and Quantum Information* (Cambridge: Cambridge University Press)

[27] Yordanov Y S and Barnes C H W 2020 Efficient quantum circuits for quantum computational chemistry arXiv:2005.14475

[28] Ryabinkin I G, Yen T-C, Genin S N and Izmaylov A F 2018 Qubit coupled cluster method: a systematic approach to quantum chemistry on a quantum computer *J. Chem. Theory Comput.* **14** 6317–26

[29] Ryabinkin I G, Lang R A, Genin S N and Izmaylov A F 2020 Iterative qubit coupled cluster approach with efficient screening of generators *J. Chem. Theory Comput.* **16** 1055–63

[30] Lang R A, Ryabinkin I G and Izmaylov A F 2020 Iterative qubit coupled cluster method with involutory linear combinations of Pauli products arXiv:2002.05701

[31] O'Gorman B, Huggins W J, Rieffel E G and Whaley K B 2019 Generalized swap networks for near-term quantum computing arXiv:1905.05118

[32] Abraham H *et al* 2019 Qiskit: an open-source framework for quantum computing (https://doi.org/10.5281/zenodo.2562110)

[33] Gard B T, Zhu L, Barron G S, Mayhall N J, Economou S E and Barnes E 2020 Efficient symmetry-preserving state preparation circuits for the variational quantum eigensolver algorithm *npj Quantum Information* **6** 1–9

[34] Sokolov I O, Barkoutsos P K, Ollitrault P J, Greenberg D, Rice J, Pistoia M and Tavernelli I 2020 Quantum orbital-optimized unitary coupled cluster methods in the strongly correlated regime: can quantum algorithms outperform their classical equivalents? *J. Chem. Phys.* **152** 124107

[35] Smart S E and Mazziotti D A 2020 Efficient two-electron ansatz for benchmarking quantum chemistry on a quantum computer *Phys. Rev. Res.* **2** 023048

[36] Sun Q *et al* PySCF: the Python-based simulations of chemistry framework *Wiley Interdisciplinary Reviews: Computational Molecular Science* vol 8 (New York: Wiley) p e1340

[37] Kraft D 1988 *A Software Package for Sequential Quadratic Programming Forschungsbericht- Deutsche Forschungs- und Versuchsanstalt fur Luft- und Raumfahrt* (Köln: Wiss. Berichtswesen d. DFVLR)

[38] Roos B O, Taylor P R and Sigbahn P E M 1980 A complete active space scf method (CASSCF) using a density matrix formulated super-CI approach *Chem. Phys.* **48** 157–73